Crystal Structure and Spectroscopic Studies of Bis(*N*-2-pyridinylcarbonyl-2-pyridinecarboximidato)copper(II) Monohydrate. Local Bonding Effects

DOLORES MARCOS, RAMON MARTINEZ-MAÑEZ, JOSE V. FOLGADO, AURELIO BELTRAN-PORTER, DANIEL BELTRAN-PORTER*

Departament de Química Inorgánica, Universitat de Valencia, Dr. Moliner 50, 46100 Burjassot, Valencia, Spain

and AMPARO FUERTES

Institut de Ciencia de Materials de Barcelona, Martí i Franqués s/n, 08028 Barcelona, Spain

(Received August 24, 1988)

Abstract

The crystal and molecular structure of bis(*N*-2-pyridinylcarbonyl-2-pyridinecarboximidato)copper-(II) monohydrate, $Cu(BPCA)_2 \cdot H_2O$, has been determined from single crystal X-ray data. It crystallizes in the monoclinic space group $P2_1/c$ with four formula units in a cell of dimensions: $a = 8.917(1)$, $b = 8.932(1)$, $c = 28.794(17)$ Å, $\beta = 95.49(2)°$. Least-squares refinement of 2754 reflections with $I > 2.5\sigma(I)$ and 379 parameters gave a final $R = 0.037$ ($R_w = 0.036$). The structure consists of discrete neutral $Cu(BPCA)_2$ entities linked two by two through water molecules hydrogen bonded to ligand carbonyl groups. The coordination geometry around copper ions can approximately be described as orthorhombically distorted octahedral. EPR and ligand field spectroscopic results have been analyzed in terms of a static Jahn–Teller distortion, and bonding parameters have been derived from EPR hyperfine and superhyperfine structures in the spectra of copper(II)-doped $Zn(BPCA)_2 \cdot H_2O$ powder samples and frozen solution.

Introduction

The Jahn–Teller effect and related phenomena concerning hexacoordinated copper(II) complexes have been the subject of a great deal of spectroscopic studies [1–4]. In particular, local effects, *i.e.* the distortions induced by copper(II) ions whose coordination polyhedra are isolated from each other in the unit cell, may usefully be investigated in complexes having general formulae $Cu(L_{III})_2X_2$, where L_{III} is a N-donor neutral tridentate rigid quasi-planar ligand such as 2,2′:6′,2″-terpyridine (terpy) or 2,4,6-tris(2-pyridyl)-1,3,5-triazine (TPT) [5–7]. In these complexes the CuN_6 polyhedra may be considered as tetragonal elongated with a slight orthorhombic component superimposed. When dealing with a given L_{III} ligand, on the basis of X-ray single crystal data and powder and single crystal EPR spectroscopic results, it has been suggested that whether the actual structure be static or dynamic is dependent on the nature of the X anion. However, the comparison of these results and those referred to other related systems does not show any concrete relation between the Jahn–Teller behaviour and the X counterions [5–10].

In this context, it has seemed interesting to us to investigate related copper(II) systems lacking X counterions, obviating in this way their possible structural influences. In this work we report the crystal structure and spectroscopic studies of the $Cu(BPCA)_2 \cdot H_2O$ compound (BPCA = *N*-2-pyridinylcarbonyl-2-pyridinecarboximidate anion). The anionic character of the BPCA has allowed us to study the effects due only to the rigid structure of the tridentate ligand. Otherwise, the $Zn(BPCA)_2 \cdot H_2O$ compound appears to be isostructural to the copper complex. Therefore, the study of the local bonding parameters in isolated CuN_6 polyhedra has been possible from the EPR results in copper(II)-doped zinc samples.

Experimental

Preparation of $Cu(BPCA)_2 \cdot H_2O$

The HBPCA ligand was isolated as described in ref. 6. When solutions of HBPCA (0.2 mmol) in acetone (2 cm^3) and $Cu(NO_3)_2 \cdot 3H_2O$ (0.1 mmol) in water (10 cm^3) were mixed with stirring, an intense blue solution resulted. The pH of this solution was slowly carried out to *ca.* 8 (with aqueous NaOH), and a green powder appeared. This was collected by filtration, washed with cold acetone and stored in a desiccator over silica gel. Single crystals were grown from slow diffusion of n-hexane into solutions of the complex in chloroform. *Anal.* Found: C, 54.3; H, 3.2; Cu, 11.6; N, 15.7. Calc. for $C_{24}H_{18}CuN_6O_5$: C, 54.0; H, 3.0; Cu, 11.9; N, 15.7%.

*Author to whom correspondence should be addressed.

0020-1693/89/$3.50

Powder samples of $Zn(BPCA)_2 \cdot H_2O$ were prepared in the same way but using $Zn(NO_3)_2 \cdot 6H_2O$ instead of copper(II) nitrate. Doped samples with *ca.* 1% Cu were obtained starting from the adequate mixture of the metallic nitrates.

Crystal Data

Green prismatic crystals of $C_{24}H_{18}CuN_6O_5$, M = 533.5, monoclinic, space group $P2_1/c$, a = 8.917(1), b = 8.932(1), c = 28.794(17) Å, β = 95.49(2)°, V = 2282.8(9) Å^3, Z = 4, D_c = 1.552 g cm^{-3}, $F(000)$ = 1092, μ(Mo Kα) = 9.48 cm^{-1}, λ(Mo Kα) = 0.70926 Å. Copper and zinc compounds are isostructural. Data for the copper complex were derived as indicated below whereas those for the zinc complex were obtained through indexation of X-ray powder diffraction patterns. This indexation leads to a = 9.02(2), b = 8.93(3), c = 28.6(3) Å, β = 96.1(3)°.

Data Collection

A well-formed crystal of dimensions 0.14 × 0.16 × 0.20 mm, was mounted on an Enraf-Nonius CAD-4 diffractometer equipped with a graphite monochromator. The cell dimensions were obtained by least-squares refinement of 25 well-centered reflections ($16° < 2\theta < 26°$). From systematic absences the space group $P2_1/c$ was assumed. Examination of four standard reflections monitored after each 50 reflections showed no substantial intensity decay. A total of 4584 reflections were measured ($2° < 2\theta < 50°$; $0 < h < 10$, $0 < k < 10$, $-34 < l < 34$) with the variable-speed ω–2θ technique, of which 2754 were unique with $I > 2.5\sigma(I)$ and used in the determination of the structure. Lorentz and polarization corrections were applied, but not for absorption.

Structure Solution and Refinement

The position of copper was determined from a tridimensional Patterson synthesis. The remaining non-hydrogen atoms were located from successive Fourier syntheses. Refinement of the structure was carried out with the SHELX76 system [11] by weighted anisotropic full-matrix least-squares methods. All hydrogen atoms were located by Fourier difference syntheses and were included in the refinement with fixed isotropic thermal parameters similar to those of the atoms to which they are bonded. The final R values were R = 0.037 and R_w = 0.036 (379 parameters refined). $\Sigma w(|F_o| - |F_c|)^2$ minimized with $w = 1/[\sigma^2(F_o) + 0.000169(F_o)^2]$ with $\sigma^2(F_o)$ from counting statistics. In the final difference map the residual maxima were less than 0.60 e Å^{-3}. Atomic scattering factors and corrections for anomalous dispersion for the copper atom were taken from International Tables for X-ray Crystallography [12]. The geometrical calculations were performed with XANADU [13] and DISTAN [14], and molecular illustrations were drawn with PLUTO [15]. Final positional parameters for non-hydrogen atoms are given in Table 1.

TABLE 1. Atomic Positional Parameters for $Cu(BPCA)_2 \cdot H_2O$[a]

Atom	x/a	y/b	z/c
Cu	0.8951(1)	0.4809(1)	0.3629(1)
O(1)	1.0883(4)	0.5633(5)	0.2436(1)
O(2)	0.7783(3)	0.4948(4)	0.2233(1)
O(3)	0.7234(4)	0.5798(3)	0.4865(1)
O(4)	0.8834(4)	0.3227(4)	0.4966(1)
N(1)	1.1153(3)	0.5610(3)	0.3662(1)
N(2)	0.9152(3)	0.5031(3)	0.2961(1)
N(3)	0.6834(3)	0.4014(3)	0.3357(1)
N(4)	0.8099(3)	0.7183(3)	0.3776(1)
N(5)	0.8600(3)	0.4720(3)	0.4303(1)
N(6)	0.9905(3)	0.2501(3)	0.3843(1)
C(1)	1.2098(5)	0.5902(5)	0.4043(2)
C(2)	1.3505(5)	0.6526(5)	0.4002(2)
C(3)	1.3930(5)	0.6846(5)	0.3570(2)
C(4)	1.2973(5)	0.6528(5)	0.3178(2)
C(5)	1.1596(4)	0.5901(4)	0.3239(1)
C(6)	1.0503(5)	0.5511(5)	0.2826(1)
C(7)	0.7927(4)	0.4754(4)	0.2649(1)
C(8)	0.6620(4)	0.4153(4)	0.2898(1)
C(9)	0.5280(5)	0.3749(5)	0.2637(2)
C(10)	0.4160(5)	0.3118(6)	0.2877(2)
C(11)	0.4391(5)	0.2938(5)	0.3349(2)
C(12)	0.5721(5)	0.3429(5)	0.3584(2)
C(13)	0.7936(5)	0.8403(5)	0.3505(2)
C(14)	0.7293(5)	0.9710(5)	0.3653(2)
C(15)	0.6776(5)	0.9753(5)	0.4082(2)
C(16)	0.6941(5)	0.8505(5)	0.4369(2)
C(17)	0.7604(4)	0.7232(4)	0.4198(2)
C(18)	0.7800(4)	0.5833(4)	0.4497(1)
C(19)	0.9042(4)	0.3484(4)	0.4566(1)
C(20)	0.9902(4)	0.2340(4)	0.4304(1)
C(21)	1.0629(5)	0.1176(5)	0.4550(2)
C(22)	1.1375(6)	0.0119(5)	0.4303(2)
C(23)	1.1370(5)	0.0272(5)	0.3833(2)
C(24)	1.0627(5)	0.1464(5)	0.3615(2)
O(w)	0.5330(5)	0.2816(5)	0.4729(2)

[a]e.s.d.s given in parentheses.

Physical Measurements

IR spectra (KBr pellets) were recorded in the 4000–250 cm^{-1} region using a Pye Unicam SP 2000 spectrophotometer. Diffuse reflectance and solution electronic spectra were recorded on a Perkin-Elmer Lambda 9 UV/VIS/NIR spectrophotometer. X-Band EPR spectra were recorded, in the temperature range 298–4.2 K, on a ER 200D Bruker spectrometer equipped with a helium cryostat. Water was determined thermogravimetrically by means of a Setaram B70 simultaneous TGA-DTA thermobalance. X-ray powder diffraction patterns ($2° < 2\theta < 50°$) were obtained by means of a Kristalloflex

810 Siemens diffractometer using Cu Kα radiation and silicon powder as internal reference.

Results and Discussion

Crystal Structure

Figure 1 shows a perspective view of the Cu-$(BPCA)_2$ units with the atomic numbering scheme, and Fig. 2 shows a stereoscopic view of the unit cell. Selected bond distances and angles are listed in Table 2. The structure consists of neutral $Cu(BPCA)_2$ entities linked two by two through hydrogen bonding involving water molecules and carbonyl groups from BPCA ligands, as shown by contact distances listed in Table 2.

Obviating the angular distortions owing to the rigidity of the BPCA ligand (see Table 2), the geometry of the CuN_6 polyhedra can be regarded as orthorhombically distorted octahedral, with an average tetragonality of 0.885. This static distortion results from the superposition of a compresion along the N(2)–Cu–N(5) axis, as the result of the rigid structure of the ligands, and an elongation along the N(4)–Cu–N(6) axis, as a consequence

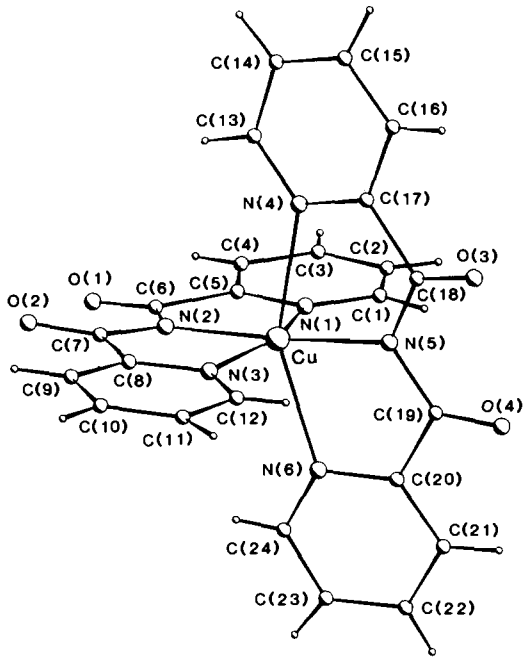

Fig. 1. Perspective view and atomic numbering of the Cu-$(BPCA)_2$ units.

TABLE 2. Bond Distances (Å) and angles (°) for $Cu(BPCA)_2 \cdot H_2O$[a]

Distances			
Cu–N(1)	2.084(3)	Cu–N(2)	1.960(3)
Cu–N(3)	2.097(3)	Cu–N(4)	2.305(3)
Cu–N(5)	1.997(3)	Cu–N(6)	2.292(3)
O(1)–C(6)	1.210(5)	O(2)–C(7)	1.204(5)
O(3)–C(18)	1.217(5)	O(4)–C(19)	1.208(5)
N(1)–C(1)	1.342(5)	N(1)–C(5)	1.342(5)
N(1)–C(20)	1.533(5)	N(2)–C(6)	1.369(5)
N(2)–C(7)	1.368(5)	N(3)–C(8)	1.322(5)
N(3)–C(12)	1.345(5)	N(4)–C(13)	1.340(5)
N(4)–C(17)	1.332(5)	N(5)–C(18)	1.373(5)
N(5)–C(19)	1.374(5)	N(6)–C(20)	1.333(5)
N(6)–C(24)	1.337(5)	C(1)–C(2)	1.388(6)
C(2)–C(3)	1.364(7)	C(3)–C(4)	1.379(7)
C(4)–C(5)	1.376(5)	C(5)–C(6)	1.504(5)
C(7)–C(8)	1.523(5)	C(8)–C(9)	1.397(5)
C(9)–C(10)	1.386(7)	C(10)–C(11)	1.366(8)
C(11)–C(12)	1.378(7)	C(13)–C(14)	1.387(6)
C(14)–C(15)	1.360(7)	C(15)–C(16)	1.386(6)
C(17)–C(18)	1.519(5)	C(19)–C(20)	1.520(5)
C(20)–C(21)	1.385(6)	C(21)–C(22)	1.390(6)
C(22)–C(23)	1.359(7)	C(23)–C(24)	1.374(6)
Angles			
N(1)–Cu–N(2)	80.5(1)	N(1)–Cu–N(3)	160.7(1)
N(1)–Cu–N(4)	90.1(1)	N(1)–Cu–N(5)	101.8(1)
N(1)–Cu–N(6)	88.4(1)	N(2)–Cu–N(3)	80.3(1)
N(2)–Cu–N(4)	98.6(1)	N(2)–Cu–N(5)	174.9(1)
N(2)–Cu–N(6)	106.8(1)	N(3)–Cu–N(4)	94.6(1)
N(3)–Cu–N(5)	97.5(1)	N(3)–Cu–N(6)	95.4(1)
N(4)–Cu–N(5)	76.9(1)	N(4)–Cu–N(6)	153.9(1)

(continued)

TABLE 1. *(continued)*

Angles			
N(5)–Cu–N(6)	77.9(1)	Cu–N(1)–C(1)	128.3(3)
Cu–N(1)–C(5)	112.5(3)	Cu–N(2)–C(6)	118.4(3)
Cu–N(2)–C(7)	118.9(2)	Cu–N(3)–C(8)	112.4(2)
Cu–N(3)–C(12)	129.0(3)	Cu–N(4)–C(13)	131.2(3)
Cu–N(4)–C(17)	110.0(2)	Cu–N(5)–C(18)	120.1(2)
Cu–N(5)–C(19)	120.2(2)	Cu–N(6)–C(20)	109.2(2)
Cu–N(6)–C(24)	132.4(3)	O(1)–C(6)–N(2)	128.5(4)
O(1)–C(6)–C(5)	119.7(4)	O(2)–C(7)–N(2)	128.9(4)
O(2)–C(7)–C(8)	120.3(4)	O(3)–C(18)–N(5)	127.6(4)
O(3)–C(18)–C(17)	118.7(3)	O(4)–C(19)–N(5)	128.0(4)
O(4)–C(19)–C(20)	118.5(3)	N(1)–C(1)–C(2)	120.7(4)
N(1)–C(5)–C(4)	122.6(4)	N(1)–C(5)–C(6)	116.6(3)
N(1)–C(20)–C(19)	118.0(3)	N(1)–C(20)–C(21)	123.1(4)
N(2)–C(6)–C(5)	111.7(3)	N(2)–C(7)–C(8)	110.8(3)
N(3)–C(8)–C(7)	117.3(3)	N(3)–C(8)–C(9)	123.2(4)
N(3)–C(12)–C(11)	121.7(5)	N(4)–C(13)–C(14)	121.9(4)
N(4)–C(17)–C(16)	122.5(4)	N(4)–C(17)–C(18)	117.4(3)
N(5)–C(18)–C(17)	113.6(3)	N(5)–C(19)–C(20)	113.5(3)
N(6)–C(24)–C(23)	123.1(4)	C(1)–N(1)–C(5)	119.2(3)
C(6)–N(2)–C(7)	122.7(3)	C(8)–N(3)–C(12)	118.6(4)
C(13)–N(4)–C(17)	118.6(4)	C(18)–N(5)–C(19)	119.4(3)
C(20)–N(6)–C(24)	117.5(3)	C(1)–C(2)–C(3)	119.6(4)
C(2)–C(3)–C(4)	119.9(4)	C(3)–C(4)–C(5)	118.0(4)
C(4)–C(5)–C(6)	120.8(4)	C(7)–C(8)–C(9)	119.5(4)
C(8)–C(9)–C(10)	117.2(5)	C(9)–C(10)–C(11)	119.7(4)
C(10)–C(11)–C(12)	119.4(5)	C(13)–C(14)–C(15)	119.3(4)
C(14)–C(15)–C(16)	119.5(4)	C(15)–C(16)–C(17)	118.0(4)
C(16)–C(17)–C(18)	120.0(4)	C(19)–C(20)–C(21)	118.9(4)
C(20)–C(21)–C(22)	118.0(4)	C(21)–C(22)–C(23)	119.1(4)
C(22)–C(23)–C(24)	119.2(4)		
Hydrogen bonding			
O(w)...O(3)′	2.941(9)	O(3)–O(w)–O(3)′	91.4(2)
O(w)...O(3)	3.161(9)	O(4)–O(w)–O(3)′	131.1(3)
O(w)...O(4)	3.151(9)	O(3)–O(w)–O(4)	50.8(3)

[a]e.s.d.s given in parentheses.

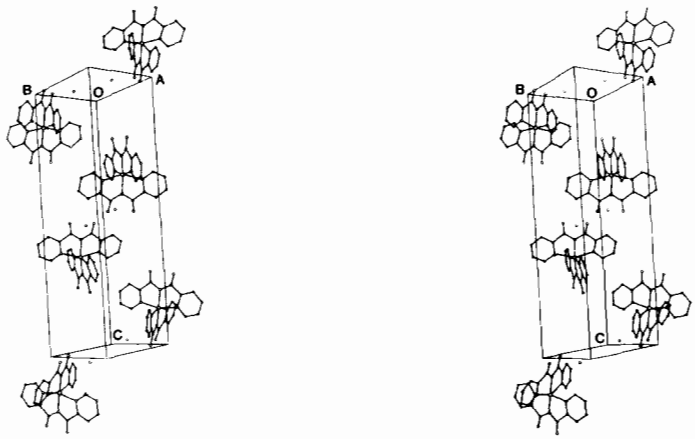

Fig. 2. Stereoscopic view of the unit cell for $Cu(BPCA)_2 \cdot H_2O$.

of the Jahn–Teller effect. A similar geometry has been previously found in the $Cu(terpy)_2(NO_3)_2$ compound [5].

The N(1), N(2), N(3) and N(5) atoms define nicely a plane (within ±0.06 Å) from which the copper atom lies 0.03 Å away. The N(2), N(4), N(5) and N(6) atoms are, however, more separated (±0.10 Å) from their least-squares plane, the copper atom being 0.04 Å apart from this plane. Both mean planes make an angle of 89.3°.

The adaptation of the BPCA ligands to the pseudo-octahedral geometry of the CuN_6 polyhedra requires deformations of the ligand framework. Both ligands are inequivalent and none of them can be considered planar. In fact, deviations of non-hydrogen atoms from the calculated mean planes become as far as 0.23 Å in one of the ligands and 0.34 Å in the other one. Furthermore, it is to be noted that the values of the angles around the carbon atoms involved in the carbonyl groups significantly differ from the idealized 120° value. Notwithstanding, as can be seen in Table 2, the experimental deformations are smaller in the ligand containing the N(4) and N(6) nitrogen atoms, *i.e.* those located farther from copper atoms. It can be stated that the need for shorter copper–nitrogen bonds introduces larger angular strains.

Infrared and Electronic Spectra

The IR spectrum of the title compound shows two noteworthy features, namely the presence of bands at 3550(m) and 3480(m) cm^{-1}, assignable to the O–H stretching vibrations of the water molecule, and that of two intense bands at 1710(vs) and 1685(vs) cm^{-1}, which are due to the C=O stretching vibrations of BPCA carbonyl groups. The shape and position of the ν(OH) bands, besides the thermoanalytical data (water is evolved endothermically at low temperature; peak temperature = 80 °C), are consistent with not clustered water molecules involved in hydrogen bonds of moderate strength [16]. The splitting of the C=O band, which appears as a unique band centered at 1750(vs) cm^{-1} in the spectrum of the HBPCA ligand [6], can be understood when the inequivalence of the two BPCA groups present in the $Cu(BPCA)_2 \cdot H_2O$ molecule is taken into account. Indeed, the band at higher wavenumber can be associated with the carbonyl groups of the more strained ligand and the band at lower wavenumber with that of the less strained BPCA group (which is that involved in the hydrogen bonds). This is supported by the observation of the unsplit carbonyl band around 1710 cm^{-1} in the IR spectra of Cu(BPCA)X complexes (X = halide or pseudohalide) containing only greatly strained BPCA ligands [17, 18]. Moreover, the IR spectrum of the $Cu(BPCA)_2$ anhydrous complex also shows two carbonyl bands at 1710 and 1695 cm^{-1}, *i.e.* only the position of the band at lower wavenumber is modified after dehydration.

Both the reflectance and solution (chloroform) spectra of the compound show two broad bands with maxima at 7800 and 14 100 cm^{-1}. These bands can be assigned to the transitions ${}_a{}^2A(x^2-y^2) \rightarrow {}_b{}^2A(z^2)$ and ${}_a{}^2A \rightarrow {}_c{}^2A$, ${}_a{}^2B$, ${}_b{}^2B$ in the C_2 symmetry of the CuN_6 polyhedra. The latter absorption corresponds to the transition to the idealized-octahedral ${}^2T_{2g}$ level, whose orbital degeneration is not lifted within the experimental band width. The position of the bands allows us to estimate the Jahn–Teller stabilization energy as 1950 cm^{-1} and the hypothetical octahedral ligand field parameter as 10 200 cm^{-1}. All these values are similar to those reported in the literature for related CuN_6 polyhedra [19, 20].

EPR Spectra

The room temperature polycrystalline powder EPR spectrum (Fig. 3a) shows a wide axial signal (140 Gauss peak-to-peak) with $g_\parallel \approx 2.24$ and $g_\perp \approx 2.06$ ($\bar{g} \approx 2.12$). When the temperature is lowered to 4.2 K the signal narrows (100 Gauss), but the g values remain practically unchanged. Accordingly, the orbital ground state of the Cu(II) would basically be $d_{x^2-y^2}$ and the CuN_6 polyhedra would be statically distorted. The observation of axial signals might seem surprising, however, in view of the orthorhombic distortion of the CuN_6 chromophores. Actually, it must be assumed that the observed $g_\perp$ value (2.06) is the mean value of the two lower components of the expected orthorhombic spectrum, which would not be resolved in X-band due to the width of the signals. In fact, both the frozen-solution (chloroform) at 100 K and the doped powder samples EPR spectra show orthorhombic signals. The g values obtained from the frozen-solution spectra (Fig. 3b) are $g_z = 2.25$, $g_y \simeq 2.10$ and $g_x = 2.03$. Given that the average g value (2.13)

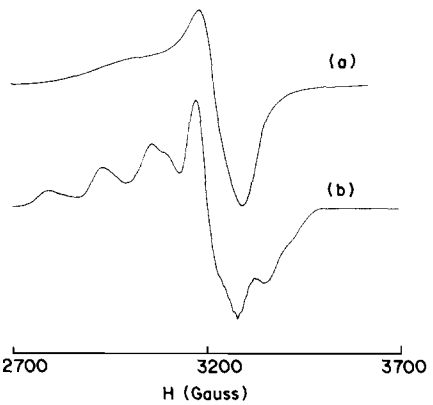

Fig. 3. X-Band EPR powder at 100 K (a) and frozen-solution (in chloroform) spectra at 100 K (b) of $Cu(BPCA)_2 \cdot H_2O$.

is practically identical with that obtained from the powder spectra, we can reasonably assume that the CuN_6 polyhedra remain unchanged in solution and the measured g values refer actually to the molecular entity. From the well resolved copper hyperfine splitting in the g_z signal we can determine $|A_z(Cu)| = 138 \times 10^{-4}$ cm^{-1}, although it is more difficult to set the $A_x(Cu)$ ($\approx 65 \times 10^{-4}$ cm^{-1}) and $A_y(Cu)$ values.

Shown in Fig. 4 are the spectra of $Zn_{1-\epsilon}Cu_\epsilon(BPCA)_2 \cdot H_2O$ powder samples ($\epsilon \approx 0.01$) recorded at various temperatures. The signals are orthorhombic, showing hyperfine and superhyperfine structures. These are well resolved at low temperatures in the g_z and g_x components. Whereas the g_x value remains practically constant from room temperature down to 4.2 K, a slight increase of both g_z and $|A_z(Cu)|$ parameters is observed as the temperature decreases (Table 3). Changes in the g_y values are more difficult to estimate. The presence of the orthorhombic spectrum already at room temperature corroborates that the CuN_6 polyhedra are statically distorted. Moreover, the whole EPR data indicates that one of the three minima in the copper(II) ground-state potential surface must significantly lower with respect to the other two [1–4]. From the constancy of the g_x value, we can conclude that the energy barrier between the lowest (z) and the highest (x) valleys must be considerably larger than the thermal energy even at room temperature. On the other hand, Silver's considerations [21] allow us to estimate the difference of energy between the two lower valleys from the temperature dependence of the g_z and g_y values. The calculated value is 196 cm^{-1}, *i.e.* close to the room temperature thermal energy.

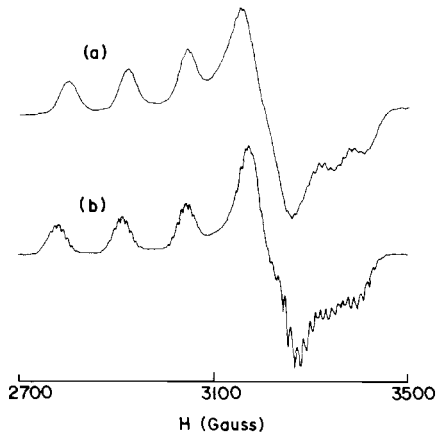

Fig. 4. X-Band EPR powder spectra of $Zn(BPCA)_2 \cdot H_2O$ doped with 1% Cu at 200 K (a) and 100 K (b).

Including some admixture of the d_{z^2} orbital because of the CuN_6 polyhedra geometry, the copper(II) ground-state wave function can be written as [22]

$$\Psi = [\sin(\phi/2)]\, d_{z^2} + [\cos(\phi/2)]\, d_{x^2-y^2} \quad (1)$$

The g values are also dependent on the vibronic coupling angular parameter ϕ

$$g_x = g_0 + 4u - 5u^2 - (2u - u^2)(\cos\phi - 3^{1/2} \operatorname{sen}\phi) \quad (2)$$

g_y and g_z coming from the above equation adding $4\pi/3$ to ϕ every time [1]. Isotropic orbital contributions $u = u_x = u_y = u_z = k^2\xi/E$ (k = covalency parameter, ξ = free ion LS-coupling parameter, E = ligand field transition to the non-resolved octahedral $^2T_{2g}$ level) have been considered. The calculated values of u and ϕ at different temperatures are listed in Table 3. Therefore, eqn. (1) becomes $\Psi = 0.14\, d_{z^2} - 0.99\, d_{x^2-y^2}$. From the u values at room temperature and 4.2 K, and E being equal to 14 100 cm^{-1}, we obtain k values of 0.74 and 0.77, respectively, *i.e.* similar to those reported for related CuN_6 polyhedra [5].

The whole molecular orbital expression for the unpaired electron of copper(II) in the studied compound is

$$\Phi = \alpha\Psi - \alpha'\Psi_L \quad (3)$$

where Ψ is the copper(II) ground-state function (from eqn. (1)) and Ψ_L is the symmetry-adapted combination of ligand s and p orbitals.

The value of α can be obtained from the well resolved hyperfine $A_z(Cu)$ component by using eqn. (4) [23]

TABLE 3. EPR Parameters for $Cu(BPCA)_2 \cdot H_2O$

Conditions	T (K)	g_x	g_y	g_z	$\lvert A_z \rvert$ (cm^{-1}) $\times 10^4$	u	ϕ(°)	α
Concentrated powder	290	2.06		2.24				
Frozen-solution	100	2.03	2.10	2.25	138.0			
Diluted powder	290	2.036	2.108	2.244	111.0	0.032	345	0.76
	200	2.036	2.101	2.254	120.6	0.033	344	0.79
	100	2.036	2.095	2.262	130.0	0.034	344	0.81
	4.2	2.036	2.092	2.265	138.0	0.035	344	0.83

$$A_z(\mathrm{Cu}) = P\{[-K - (4/7)\cos\phi]\alpha^2 + (6u/7)\cos\phi + 8u\cos^2(\phi/2)\} \quad (4)$$

Assuming a negative sign for $A_z(\mathrm{Cu})$, and from the u, ϕ and A_z values at various temperatures, we obtain the α values shown in Table 3. Calculations have been performed considering $P = 0.036$ cm^{-1} and $K = 0.43$ [3].

The coefficient α' is accessible from the nitrogen SHF structure in the EPR spectra. Thus in the g_z part of the spectra at temperatures lower than 200 K, a nine-line SHF structure is observed, giving a coupling constant of 9×10^{-4} cm^{-1}. This structure is accountable in terms of the equivalence, in that concerning the SHF splitting, of the four equatorial nitrogen atoms. The axial nitrogen atoms are assumed to be SHF inactive because the copper(II) ground-state is predominantly $d_{x^2-y^2}$. The analysis of the g_x part is intricate but coupling constants of 13 and 9×10^{-4} cm^{-1} may be roughly derived. Since the principal direction of the ^{14}N tensor is along the Cu–N bond, the following set of SHF parameters results

$$A_x(\mathrm{N}) = A_y(\mathrm{N}) = A_\perp(\mathrm{N}) = 9 \times 10^{-4}\ \mathrm{cm}^{-1}$$

$$A_z(\mathrm{N}) = A_\parallel(\mathrm{N}) = 13 \times 10^{-4}\ \mathrm{cm}^{-1}$$

Hence, since

$$A_\parallel = A_{\mathrm{iso}} + 4/5A_{\mathrm{ani}}$$

$$A_\perp = A_{\mathrm{iso}} - 2/5A_{\mathrm{ani}} \quad (5)$$

we obtain $A_{\mathrm{iso}} = 10.3 \times 10^{-4}$ cm^{-1} and $A_{\mathrm{ani}} = 3.3 \times 10^{-4}$ cm^{-1}.

While the isotropic part of the coupling constants is due to the s-electron density at the ^{14}N nucleus, the p-electron density contributes only to the anisotropic part [22]

$$A_{\mathrm{iso}} = A^{\mathrm{s}}_{\mathrm{N}} c_{\mathrm{s}}^2$$

$$A_{\mathrm{ani}} = A^{\mathrm{p}}_{\mathrm{N}} c_{\mathrm{p}}^2 \quad (6)$$

where c_{s} and c_{p}, the MO coefficients of the 2s and 2p orbitals of the nitrogen, are directly related to α'. Thus, using the standard values of $A^{\mathrm{s}}_{\mathrm{N}}$ and $A^{\mathrm{p}}_{\mathrm{N}}$ [3], we find $c_{\mathrm{s}} = 0.139$ and $c_{\mathrm{p}} = 0.287$. Given that $c_{\mathrm{s}}^2 + c_{\mathrm{p}}^2 = 0.10169$ must be equal to $\alpha'^2/4$, a value of $\alpha' = 0.64$ results.

Finally, because the d_{z^2} contribution to Ψ can be neglected in the first approximation, the ligand function will be [22]

$$\Psi_{\mathrm{L}} = 1/2(-\sigma_1 + \sigma_2 + \sigma_3 - \sigma_4)$$

$$\sigma_i = np_i + (1 - n^2)^{1/2} s_i \quad (7)$$

and the following complete ground state function can be written

$$\Phi = 0.83\, d_{x^2-y^2} - 0.64[0.90/2(-p_1 + p_2 + p_3 - p_4) + 0.44/2(-s_1 + s_2 + s_3 - s_4)] \quad (8)$$

It is to be noted that this function has been simplified by obviating the chemical differences among the in-plane nitrogen atoms. Actually, the relative contributions of the nitrogen 2s and 2p orbitals set (*ca.* 20% and 80%, respectively, according to the $c_{\mathrm{s}}/c_{\mathrm{p}} \approx 0.5$ ratio) must be considered as the average of those corresponding to the two pyridine and the two imidate nitrogen atoms. For the first ones, it is reasonable to assume relative s/p = 1/2 contributions (*i.e.* 33% s and 66% p, respectively). For the second ones, because of the presence of two unshared electron pairs on each donor atom, a p contribution to the bonding orbital ranging from 66% to 100% may be expected. The experimental average values suggest that the imidate nitrogen contribution to the MO function is essentially of p-type, as could have been predicted from Bent's isovalence concept [24].

Conclusions

The structure of $Cu(BPCA)_2 \cdot H_2O$ provides a new example of the energetic preference of the elongated coordination mode rather than the compressed one, in Jahn–Teller distorted octahedral copper(II) complexes.

On the other hand, a feature of $Cu(BPCA)_2 \cdot H_2O$ to be emphasized is the static character of the $[CuN_6]$ chromophore. In fact, $[CuN_6]$ chromophores are dynamic in most of the well known related systems [5–10]. That differentiating the literature cases from the now studied one is the spatial electronic charge distribution around copper(II) ions. Actually, it is reasonable to think that, for species containing $[CuN_6]^{2+}$ type ions, the electronic potential around copper due to the set of X-counterions be quasi-isotropic and has a smooth gradient. Therefore, the different possible configurations of the chromophores would have analogous energy values. This would also result, very likely, in low values of the barriers of energy among the Jahn–Teller wells. Then, the thermal energy would render possible transitions between the wells and a dynamic behaviour would result. On the contrary, anionic ligands which give rise to neutral $[CuN_6]$ entities would originate anisotropic and sharp-gradient electrostatic potentials. Accordingly, one of the possible configurations would be preferred and a static behaviour would be observed.

Finally, the spectroscopic data are consistent with the static distortion of the CuN_6 chromophores, and EPR spectroscopy on diluted samples has proved again to be a suitable technique for studying the MO parameters for the Cu–N bonds in such systems.

The experimental values of the hyperfine parameters can come about through both the relatively low contribution of the d_{z^2} orbital to the copper(II) ground state and the considerable density of unpaired spin onto the ligands.

Supplementary Material

Tables of anisotropic thermal parameters and observed and calculated structural factors can be obtained from the authors upon request.

Acknowledgements

This work was supported by a grant of CAICYT which we acknowledge. A.F., J.V.F. and R.M. thank the CSIC, MEC and Generalitat Valenciana, respectively, for research fellowships. We are grateful to Dr C. Miravitlles for making available the Enraf-Nonius CAD-4 diffractometer.

References

1 D. Reinen and C. Friebel, *Struct. Bonding (Berlin), 37* (1979) 1.
2 B. J. Hathaway, *Coord. Chem. Rev., 41* (1982) 423, and refs. therein.
3 A. Ozarowski and R. Reinen, *Inorg. Chem., 24* (1985) 3860.
4 M. J. Riley, M. A. Hitchman and D. Reinen, *Chem. Phys., 102* (1986) 11.
5 R. Allmann, W. Henke and R. Reinen, *Inorg. Chem., 17* (1978) 378.
6 J. V. Folgado, *Ph.D. Thesis,* Universidad de Valencia, Spain, 1987.
7 M. I. Arriortua, T. Rojo, J. M. Amigo, G. Germain and J. P. Declercq, *Acta Crystallogr., Sect. B, 38* (1982) 1323.
8 B. J. Hathaway, *Coord. Chem. Rev., 36* (1981) 325, and refs. therein.
9 J. H. Ammeter, H. B. Burgi, E. Gamp, V. Meyer-Sandrin and W. P. Jensen, *Inorg. Chem., 18* (1979) 733.
10 J. S. Wood, C. P. Keijzers, E. de Boer and A. Buttafava, *Inorg. Chem., 19* (1980) 2213.
11 G. M. Sheldrick, *SHELX76,* program for crystal structure determination, Cambridge University, 1976.
12 *International Tables for X-Ray Crystallography,* Vol. 4, Kynoch Press, Birmingham, 1974, pp. 72–99.
13 P. Roberts and G. M. Sheldrick, *XANADU,* program for crystallographic calculations, Cambridge University, 1975.
14 J. Burzlaff, V. Bohme and M. Gomm, *DISTAN,* University of Erlangen, F.R.G., 1977.
15 W. D. S. Motherwell and W. Clegg, *PLUTO78,* program for plotting molecular and crystal structures, Cambridge University, 1978.
16 J. R. Ferraro, *Low-Frequency Vibrations of Inorganic and Coordination Compounds,* Plenum, New York, 1971, p. 65.
17 J. V. Folgado, E. Escrivá, A. Beltrán-Porter and D. Beltrán-Porter, *Transition Met. Chem., 12* (1987) 306.
18 J. V. Folgado, E. Coronado, D. Beltrán-Porter, R. Burriel, A. Fuertes and C. Miravitlles, *J. Chem. Soc., Dalton Trans.,* (1988) 3041.
19 D. Reinen, A. Ozarowski, B. Jakob, J. Pebler, H. Stratemeier, K. Wieghardt and I. Tolksdorf, *Inorg. Chem., 26* (1987) 4010.
20 P. Chaudhuri, K. Oder, K. Wieghardt, J. Weiss, J. Reedijk, W. Hinrichs, J. Wood, A. Ozarowski, H. Stratemeier and D. Reinen, *Inorg. Chem., 26* (1987) 4010.
21 B. L. Silver and D. Getz, *J. Chem. Phys., 61* (1974) 638.
22 A. Abragam and B. Bleaney, *Electron Paramagnetic Resonance of Transition Ions,* Clarendon, Oxford, 1970, p. 761.
23 A. Bencini, I. Bertini, D. Gatteschi and A. Scozzafava, *Inorg. Chem., 17* (1978) 3194.
24 K. F. Purcell and J. C. Kotz, *Inorganic Chemistry,* W. B. Saunders, Philadelphia, 1977, p. 109.